FULL FIELD STRAIN ASSESSMENT OF SINGLE LAYER UD-NCF DURING DRAPING PROCESS

Ghazimoradi, Mehdi[1]*, Montesano, John[1]
[1] Composites Research Group, Department of Mechanical & Mechatronics Engineering, University of Waterloo, 200 University Ave. West, Waterloo N2L 3G1, Canada
* Mehdi Ghazimoradi (Mehdi.ghazimoradi@uwaterloo.ca)

Keywords*: Unidirectional non crimp fabrics (UD-NCF), formability, strain contours*

ABSTRACT

This experimental study focused on the formability of a polyester stitch bonded carbon fiber (CF) heavy tow unidirectional non-crimp fabric (UD-NCF). Hemispherical draping tests were performed to investigate the deformation of the fabric when loaded from both sides (i.e., the side with the tricot stitching pattern, and the transverse supporting glass fiber (GF) yarn side). A 50 mm radius hemispherical punch was used along with a steel ring binder to hold the fabric specimen onto the die during draping. Tests were performed at room temperature and under quasi-static conditions with a vertical punch speed of 1.0 mm/s. A 3D digital image correlation (DIC) system was used to capture and analyze deformation images of the fabric and to determine the corresponding strain contours. The main defects were observed to be local in-plane buckling of the tows and macroscopic wrinkling of the fabric. The measured full field strain contours at the final stage of forming showed that in-plane shear deformation was greatest in the region of the specimens where more wrinkling was observed. Comparison of the force-displacement response of the UD-NCF when loaded from both sides revealed that there were no distinguishable differences.

1 INTRODUCTION

During the last decade, unidirectional non crimp fabrics (UD-NCFs) with unique tow and stitching architectures have been developed and used as reinforcements in high-performance composite materials fabricated using liquid composite molding processes [1,2]. UD-NCFs have been widely applied in various industries such as aeronautic, automotive and wind energy due to good drapability and ease of handling during processing [3–7]. However, compared to other engineering fabrics the deformation and formability characteristics of UD-NCFs have not been extensively investigated [8,9]. Capturing the local and macroscopic deformation characteristics of fabrics during forming is important to understand the mechanisms that cause defects, while also enabling multiscale validation of draping simulation models. Forming defects for UD-NCFs that have been observed include local buckling of the tows and macroscopic wrinkling of the fabric [8].

Three-dimensional digital image correlation (3D-DIC) has been widely used to capture surface deformations and to determine the associated full-field strains for cases when out-of-plane displacements of test specimens are not negligible. The 3D-DIC technique has also been demonstrated to be suitable for investigating the local and macroscopic deformation characteristics of textile reinforcements. Lomov et al. [10] used 3D-DIC to track the local deformations of a single layer of woven fabric after a hemispherical draping test , leading to the determination of the local fiber orientations and shear angles. Moreover, 3D-DIC data was used as input data for the validation of material draping models and for the prediction of the consolidated part performance via structural finite element

analysis. Pazmino et al. [11] studied the formability of a non-crimp 3D orthogonal woven fabric reinforcement and compared the deformation results from two different commercial image correlation software programs, namely VIC-3D and MatchID3D. A comparison of the displacement and shear angle distributions determined by both software for the reinforcement shaped on tetrahedral and double-dome moulds were in good agreement.

In the current paper, an experimental investigation on forming of a UD-NCF was conducted by utilizing a hemispherical draping test. In particular, the shear strain distribution during the test was measured by means of Vic-3D DIC analyses, while defects were observed. The corresponding force-displacement response was also captured.

2 MATERIAL

A commercially available UD-NCF, namely Zoltek™ PX35-UD300, was investigated. The heavy-tow fabric comprised 5 mm wide tows each containing 50,000 PX35 carbon fiber (CF) filaments. The tows were aligned parallel to each other and stitched together with polyester yarn (76 dtex) in a tricot pattern (Figure 1a). The supporting glass fiber (GF) yarns (34 dtex) were aligned perpendicular to the CF tows, positioned between the CFs and the polyester stitching (Figure 1b). A light thermosetting binder powder was uniformly distributed on the stitching side of the fabric. The total fabric areal density was 333 g/m^2 with the carbon fiber tows accounting for 92.8% of the total weight. All test specimens used in this study were cut from one roll of the UD-NCF fabric. Some features of the UD-NCF are listed in Table 1.

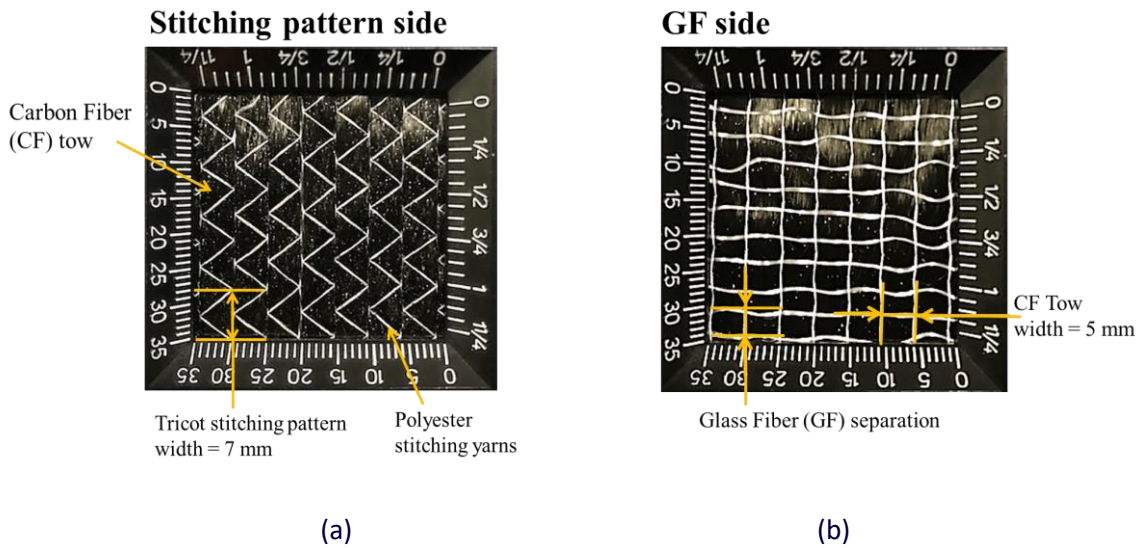

Figure 1. Images of Zoltek™ PX35-UD300 unidirectional non-crimp fabric: (a) stitching pattern side and (b) glass fiber side

Table 1. Zoltek™ PX35-UD300 unidirectional non-crimp fabric characteristics

Parameter	Value
Glass fiber yarn weight fraction	3.0 %
Glass fiber yarn linear density	34 dtex
Polyester stitch weight fraction	1.8 %
Polyester stitch linear density	76 dtex
Binder resin powder weight fraction	2.4 %
Carbon fiber tow weight fraction	92.8 %
Nominal Carbon fiber diameter	7.2 µm

3 DRAPING TEST FOR UD-NCF

Single-layer hemispherical draping tests were performed on 600 mm X 600 mm UD-NCF specimens using the set-up illustrated in Figure 2. A 50 mm radius steel hemispherical punch was used to drape the fabric, while a steel ring with a 125 mm inner diameter, 20 mm width, 4 mm thickness, and a mass of 259 g was used to hold the fabric onto the die during draping (Figure 2). The die was made from a transparent PVC plate to allow for observation of the fabric during draping. Tests were performed at room temperature and under quasi-static conditions with a vertical punch speed of 1 mm/s. The deformation of the fabric during forming was measured by a 3D DIC system (described in Section 4). Two sets of draping tests were performed with the punch in contact with the stitching side and GF yarn side of the fabric. Three repeats were performed for both sets of draping tests.

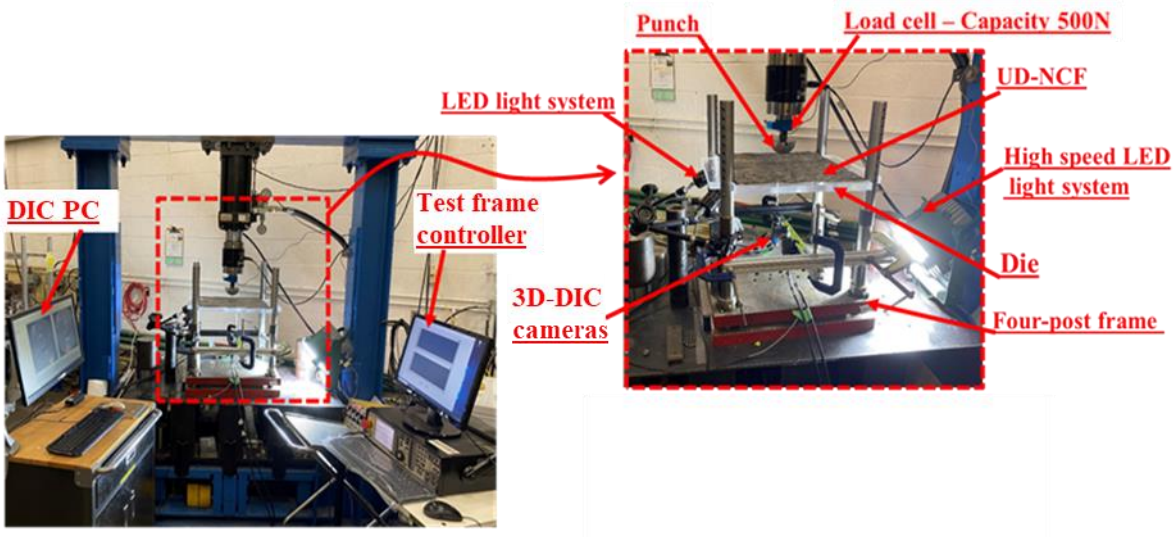

Figure 2. Hemispherical test setup for single layer of UD-NCF.

4 DIGITAL IMAGE CORRELATION FOR DRAPING TEST

One surface of the fabric specimens was randomly speckled with white oil-based paint to provide a clear contrast with the fabric for DIC analysis. A pair of cameras with 17 mm focal length lenses operated at a frame rate of 30 frames per second captured the specimen deformation images from the far side of the punch (Figure 2). The 3D-DIC software Vic 3D (Correlated Solutions Inc.) was used during the draping tests to process the captured images. The analysis was performed on the complete test specimen surface to generate strain contour plots, and within 50 × 50 mm^2 (200 × 200 pixel^2) regions of interest (ROIs) on the specimens to record average strain magnitudes. A step size of 5–11 pixels, a subset size of 31–55 pixels and strain filter size of 9 was used in the software for all specimens. To increase the correlation capacity of the system given the large deformations expected, the incremental correlation option was activated.

5 RESULTS AND DISCUSSION

For a specimen loaded on the GF side, local tow buckling and macroscopic wrinkling were typically observed in two regions on the formed specimen (see region i and region ii in Figure 3a). Both defects were predominantly induced by local transverse compressive deformation of the carbon fiber tows and the accompanying tow gapping, which was primarily caused by deformation of the stitching web during in-plane shear deformation of the fabric. Local buckling of the CF tows was induced by axial compression on many of the stitching segments crossing the tows during shearing of the fabric, which reduced the support of the CF tows causing them to buckle in-plane. Macroscopic wrinkling was caused by shear-induced CF tow gapping, which caused the fabric to bend along the direction of the GF yarns under transverse compression. Region i exhibited more macroscopic wrinkling as a result of higher observed local shear strains (Figures 3b-c) and transverse compressive strains.

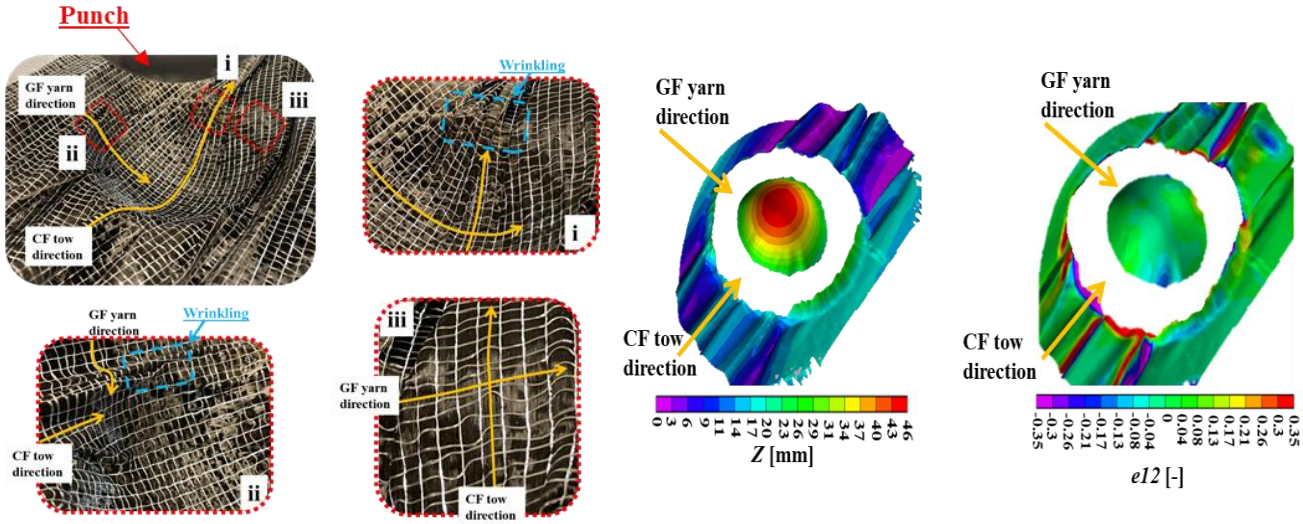

Figure 1. Deformation of the UD-NCF specimen loaded on the GF yarn side during hemispherical punch forming at a punch displacement of 46 mm: (a) defects on the fabric GF yarn side in three different directions, (b-c) contour maps of displacement (Z) and shear strain (e_{12}) on the fabric stitching side.

The shear strain distribution across the surface of the single layer specimen (stitching side) was assessed at a punch displacement of 46 mm (Figure 3c). The highest shear strain was captured in region i, whereas the minimum shear strain was observed at the specimen center. The peak shear strain in region i along the CF tow direction was approximately 0.35 mm/mm, which is the reason for a high degree of wrinkling in this region.

When loading the specimens on the stitching side, there was no discernable differences on the type or location of defects observed (Figure 4a) or the shear strain contour (Figure 4c) when compared to the specimens loaded on the GF side. This may be due to the fact that the fabric/steel has a similar friction coefficient at room temperature (which was measured by Trejo [12]) for both sides of the fabric.

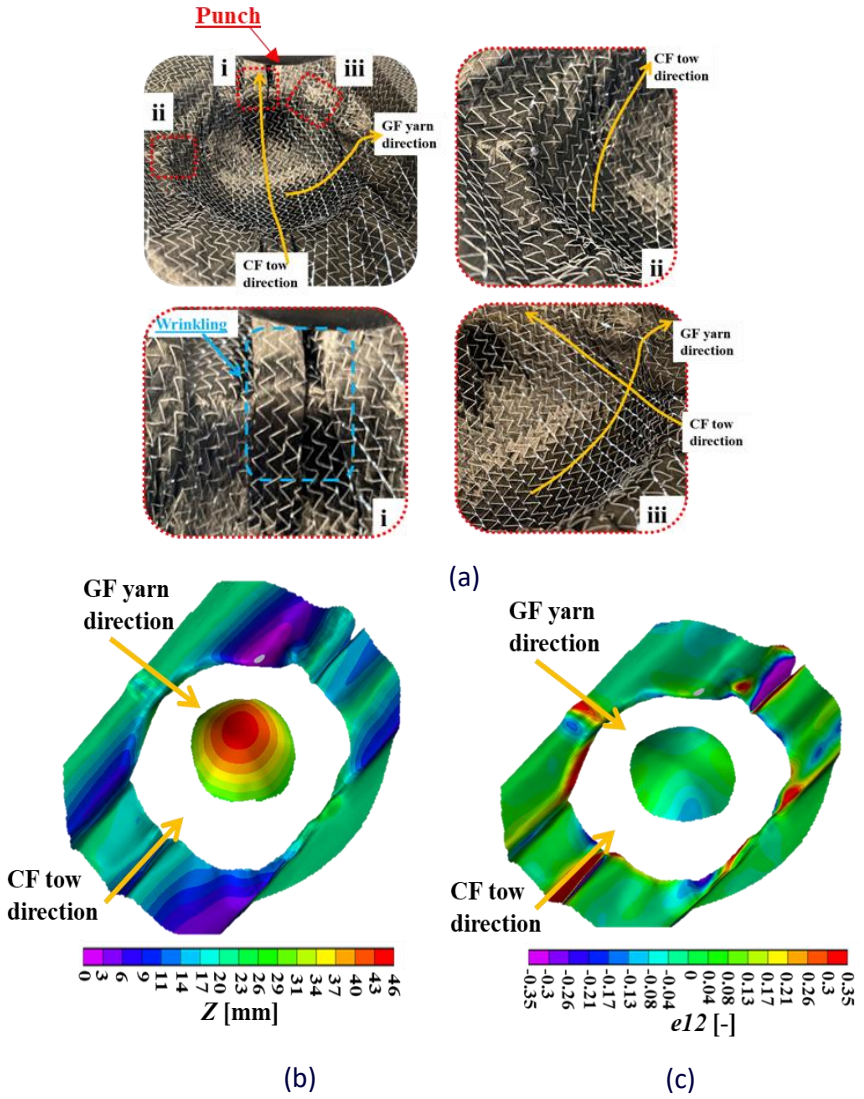

Figure 2. Deformation of the UD-NCF specimen loaded on the stitching side during hemispherical punch forming at a punch displacement of 46 mm: (a) defects on the fabric stitching side in three different directions, (b-c) contour maps of displacement (Z) and shear strain (e_{12}) on the fabric GF yarn side.

The force-displacement response for UD-NCF specimens loaded on both sides (stitching side and GF yarn side) is shown in Figure 5. Up 15 mm punch displacement, the response is consistent. After 46 mm of punch displacement, the average load response on the GF side was 5 N lower than the average load on the stitching side. However, by considering the data scatter bars, the load response of the stitching side of the specimen is within the observed data variability of the GF yarn side of the specimen, and this implies that the loading response of both sides of the fabric is similar at 46 mm of punch displacement.

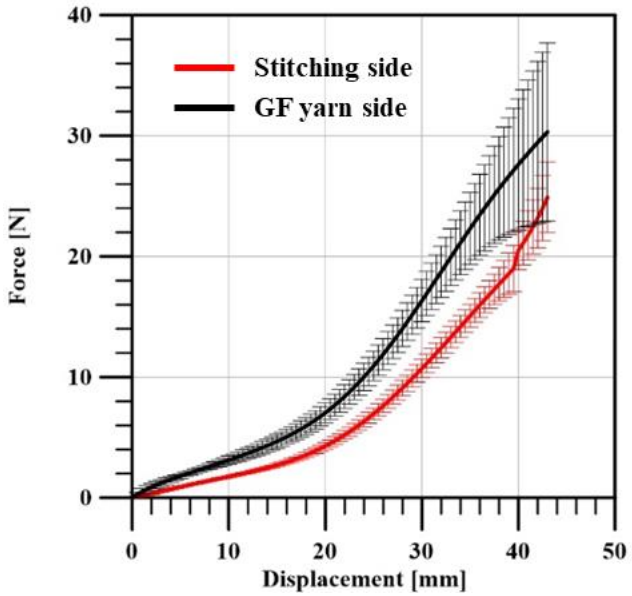

Figure 5. Force-displacement response of both side (stitching side and GF yarn side) of UD-NCF.

6 CONCLUSION

The purpose of this study was to capture the full field strain maps of unidirectional non-crimp fabric (UD-NCF) during single layer hemispherical draping tests and relate to the observed defects. A three-dimensional digital image correlation (3D-DIC) setup was used to capture deformation of the fabric specimens, while commercial software Vic 3D was used to determine the full field strain maps. The main defects observed during the tests were local buckling of the tows and macroscopic wrinkling of the fabric, which was consistent when the fabric was loaded from both sides. Local tow buckling and macroscopic wrinkling were both driven by shear deformation of the fabric and the associated deformation of the stitching. For the former, axial compression of stitching segments led to instability of the tows which caused in-plane buckling, while for the latter shear-induced tow gapping and transverse compressive strains promoted bending of the fabric. The measured full field shear strain component contours at the final stage of forming showed that the specimen center exhibited the minimum shear strain, and the highest shear strain was observed in the region near the die/punch clearance where the greatest number of wrinkles were observed.

7 REFERENCES

[1] Rouf K, Worswick MJ, Montesano J. A multiscale framework for predicting the mechanical properties of unidirectional non-crimp fabric composites with manufacturing induced defects. J Compos Mater 2021;55:741–57. https://doi.org/10.1177/0021998320958189.

[2] Cherniaev A, Zeng Y, Cronin D, Montesano J. Quasi-static and dynamic characterization of unidirectional non-crimp carbon fiber fabric composites processed by HP-RTM. Polym Test 2019. https://doi.org/10.1016/j.polymertesting.2019.03.036.

[3] Ghazimoradi M, Carvelli V, Montesano J. Assessing the Multiaxial Deformation Response of Unidirectional Non-Crimp Fabrics. Proc Am Soc Compos-Sixth Tech Conf Compos Mater 2021. https://doi.org/10.12783/asc36/35914.

[4] Trejo A, Ghazimoradi M, Butcher C, Montesano J., Characterization of the Shear Response of Unidirectional Non-Crimp Carbon Fiber Fabrics",11th Canadian-International Conference on Composites, Kelowna, British Columbia, Canada 2019.

[5] Trejo EA, Ghazimoradi M, Butcher C, Montesano J. Assessing strain fields in unbalanced unidirectional non-crimp fabrics. Compos Part A Appl Sci Manuf 2020;130. https://doi.org/10.1016/j.compositesa.2019.105758.

[6] Chen S, McGregor OPL, Harper LT, Endruweit A, Warrior NA. Defect formation during preforming of a bi-axial non-crimp fabric with a pillar stitch pattern. Compos Part A Appl Sci Manuf 2016. https://doi.org/10.1016/j.compositesa.2016.09.016.

[7] Ghazimoradi M, Trejo EA, Butcher C, Montesano J. Characterizing the macroscopic response and local deformation mechanisms of a unidirectional non-crimp fabric. Compos Part A Appl Sci Manuf 2022;156:106857. https://doi.org/10.1016/j.compositesa.2022.106857.

[8] Ghazimoradi M, Trejo EA, Carvelli V, Butcher C, Montesano J. Deformation characteristics and formability of a tricot-stitched carbon fiber unidirectional non-crimp fabric. Compos Part A Appl Sci Manuf 2021;145:106366. https://doi.org/10.1016/j.compositesa.2021.106366.

[9] Schirmaier FJ, Weidenmann KA, Kärger L, Henning F. Characterisation of the draping behaviour of unidirectional non-crimp fabrics (UD-NCF). Compos Part A Appl Sci Manuf 2016. https://doi.org/10.1016/j.compositesa.2015.10.004.

[10] Lomov SV, Boisse P, Deluycker E, Morestin F, Vanclooster K, Vandepitte D, et al. Full-field strain measurements in textile deformability studies. Compos Part A Appl Sci Manuf 2008;39:1232–44. https://doi.org/10.1016/j.compositesa.2007.09.014.

[11] Pazmino J, Carvelli V, Lomov SV, Van Mieghem B, Lava P. 3D digital image correlation measurements during shaping of a non-crimp 3D orthogonal woven E-glass reinforcement. Int J Mater Form 2014;7:439–46. https://doi.org/10.1007/s12289-013-1139-6.

[12] Trejo EA. Characterizing the deformation response of a unidirectional non-crimp fabric for the development of computational draping simulation models. University of Waterloo, 2020.